

Optimization of the Cherenkov signal from TeO₂ bolometers.

N. Casali^{1,2 a}

¹ Dipartimento di Fisica - Sapienza Università di Roma, Piazzale Aldo Moro 2, 00185, Roma - Italy

² INFN - Sezione di Roma, Piazzale Aldo Moro 2, 00185, Roma - Italy

Received: date / Revised version: date

Abstract. The most sensitive process able to probe the Majorana nature of neutrinos and discover Lepton Number Violation is the neutrino-less double beta decay ($0\nu\text{DBD}$). A novel approach able to improve the sensitivity of the current bolometric experiments searching for this rare nuclear decay is the α background rejection. In TeO₂ bolometers the α particles rejection can be performed tagging the Cherenkov light emitted only by electrons. This approach was tested in several works which demonstrated the feasibility of this technique but, on the other hand, the amount of Cherenkov light detected was lower with respect to the expected one, undermining the complete rejection of α background.

In this paper we compare the results obtained in these works with a detailed Monte Carlo simulation able to reproduce the number of Cherenkov photons produced in β/γ interactions within the TeO₂ bolometer and their propagation in the experimental set-up. We demonstrate that the light yield detectable from a $5 \times 5 \times 5 \text{ cm}^3$ TeO₂ bolometer can be increased up to 58% with respect to the one measured by the current R&D detectors increasing the surface roughness of the crystal and improving the light detector design.

Moreover taking into account the intrinsic fluctuations of the number of Cherenkov photons we study the possibility to disentangle β from γ interactions that represent the ultimate background source. Unfortunately this discrimination is not feasible.

PACS. 23.40.-s Double β decay – 14.60.Pq Neutrino mass and mixing – 07.57.Kp Bolometer – 41.60.Bq Cherenkov radiation – 05.10.Ln Monte Carlo methods

1 Introduction

CUORE (*Cryogenic Underground Observatory for Rare Events*) [1] is an array of 988 TeO₂ bolometers of $5 \times 5 \times 5 \text{ cm}^3$ each, and it will become the most sensitive experiment searching for $0\nu\text{DBD}$ of ^{130}Te . The signal produced by this reaction are two electrons with a total kinetic energy of 2.527 MeV. Unfortunately the α background rate, at the level of 0.01 counts/keV/kg/y, will limit the sensitivity on the searched process and, consequently on the effective Majorana mass ($m_{\beta\beta}$). The sensitivity on $m_{\beta\beta}$ will be at the level of $0.05 \div 0.13 \text{ eV}$, i.e. the beginning of the inverted hierarchy region of the neutrino masses. Next generation $0\nu\text{DBD}$ experiments, such as CUPID [2], aims to reach a sensitivity on $m_{\beta\beta}$ at a level of 0.01 eV, i.e. the end of the inverted hierarchy region. To reach this ambitious goal the source mass must be increased and the background in the region of interest dramatically reduced. To increase the number of $0\nu\text{DBD}$ emitters, crystals grown with enriched material are needed. The background suppression can be achieved rejecting the α particle interactions originating from the radioactive contaminations located in the surfaces of the detector components. Since no scintillation process exists in TeO₂ crystal [3,4] and also no difference exists between the pulses shape produced by α and β/γ interactions [5], the only possibility to achieve the background suppression is exploiting the Cherenkov light emitted in TeO₂ crystals only by β/γ interactions [6,7]. Coupling a sensitive cryogenic light detector to the TeO₂ bolometer is possible to reject the α background, since the velocity of the α particles is below the Cherenkov threshold.

In order to measure the Cherenkov light yield (LY) of TeO₂ bolometers several tests coupling germanium light detectors [8] were performed in a dilution refrigerator working at 10 mK located deep underground in the Hall C of Laboratori Nazionali del Gran Sasso. The first result that probed the feasibility of this technique to reject the α background can be found in Ref. [9] where a small TeO₂ crystal ($3.0 \times 2.4 \times 2.8 \text{ cm}^3$) covered with VM2002 reflective foils was faced to a germanium light detector: the amount of Cherenkov light detected at the Q-value of ^{130}Te $0\nu\text{DBD}$

Send offprint requests to:

^a e-mail: nicola.casali@roma1.infn.it

(2527 keV) was about 173 eV. A more systematic study of the Cherenkov LY emitted by a CUORE-size TeO₂ crystal has been done in Ref. [10] where several reflectors and detector configurations were tested in order to optimize the photons collection. The result of this study was that the maximum amount of Cherenkov light detected from a CUORE TeO₂ crystal is about 100 eV at 0νDBD, irrespective of the reflector. Summing up the tiny amount of the Cherenkov light detected combined with the poor baseline resolution of the light detectors (80 eV RMS) prevented the complete α particles rejection. These measurements also highlighted a significant difference between the detected Cherenkov signal and the expected one [10].

The purpose of this paper is to determine, exploiting a detailed Monte Carlo simulation of the Cherenkov photons production and propagation, why the amount of the expected Cherenkov light and the detected one are so different, and why none of the trials performed in Ref. [10] succeeded in providing a significant increase of the light collection efficiency. In addition, we identify the parameters able to improve the light collection efficiency. Finally we demonstrate that the Cherenkov radiation tagging technique does not allow the discrimination between β and γ interactions, that will constitute the ultimate background source for the bolometric experiments based on TeO₂ crystals.

2 Cherenkov photons production in tellurium dioxide crystal

The number of Cherenkov photons produced per unit path length and per unit wavelength of a particle with charge ze and velocity $v = \beta c$ is [11]:

$$\frac{dN^2}{dx d\lambda} = \frac{2\pi\alpha z^2}{\lambda^2} \left(1 - \frac{1}{\beta^2 n^2(\lambda)} \right) \quad (1)$$

where α is the fine-structure constant, λ the wavelength of the Cherenkov photons and $n(\lambda)$ the refractive index of the material. As shown in Eq. 1 the evaluation of the number of Cherenkov photons produced by a particle interaction within a TeO₂ crystal requires the knowledge of its optical properties and the particle range. Therefore in the following sections the optical properties of TeO₂ crystal will be presented together with its stopping power for electrons, in order to perform an estimation of the Cherenkov photons emitted in the β/γ interaction.

2.1 Optical properties of TeO₂ crystal

The TeO₂ crystal is a birefringent material. The ordinary and extraordinary refractive indices (n_o and n_e , respectively) are shown in Fig. 1. Both the refractive indices are described by the Sellmeier equation [13]:

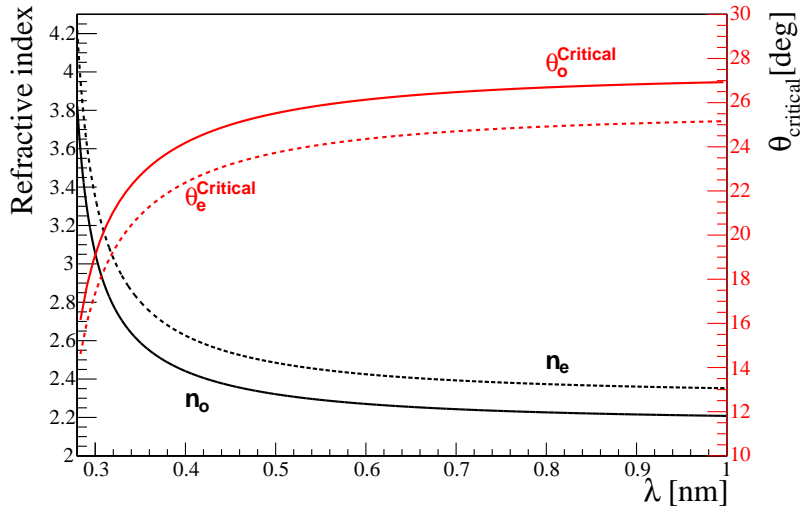


Fig. 1. Ordinary (continuous black line) and extraordinary (dotted black line) refractive indices of TeO₂ crystal as function of wavelength at room temperature [12]. $\theta_{Critical}$ values for an optical photon that hits the internal surface of a TeO₂ crystal surrounded by vacuum using the ordinary (continuous red line) and extraordinary (dotted red line) refractive indices.

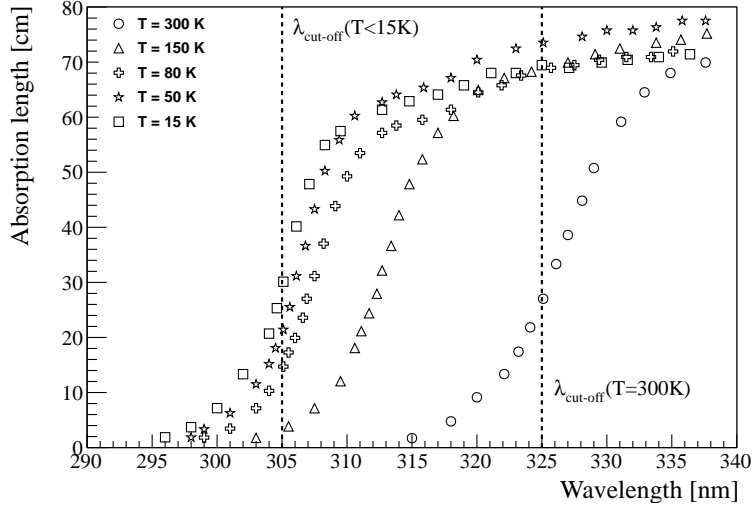
$$n(\lambda)^2 - 1 = \frac{A\lambda^2}{\lambda^2 - \lambda_1^2} + \frac{B\lambda^2}{\lambda^2 - \lambda_2^2} \quad (2)$$

	A	λ_1 [μm]	B	λ_2 [μm]
n_o	2.584	0.1342	1.157	0.2638
n_e	2.823	0.1342	1.542	0.2631

Table 1. Coefficients of the Sellmeier equations for the TeO₂ crystal at room temperature [12].

The Sellmeier parameters for the TeO₂ crystal are shown in Table 1.

As TeO₂ crystals are currently produced for acousto-optic devices, special attention is given in literature only to optical properties connected to this application. The study of optical characteristics as transmission and reflection near and above the fundamental absorption edge, at low temperatures, were carried out down to only 80 K [14] and experimental results [14,12] do not allow for a definitive interpretation of electronic band structure for TeO₂ crystal. It is also missing from the literature a detailed study of the agreement between calculated electronic structure [15] and optical transmission measurements. We performed optical transmission measurements on pure TeO₂ slices using

**Fig. 2.** Absorption length ($\delta(\lambda)$) for different temperatures around the fundamental absorption edge.

a Perkin Elmer Lambda 900 spectrophotometer and a Leybold RDK10-320 ($T_{\min}=12$ K) cryostat. The results around the fundamental absorption edge are shown in Fig. 2; for wavelengths greater than 340 nm the absorption length approaches a value of about 80 cm, irrespective of the temperature. The absorbance spectra show a temperature dependence typical of an indirect band structure, and the shift in the $\lambda_{cut-off}$ (defined as the inflection point of the curve) due to the temperature variation reaches an asymptotic value for $T < 50$ K. This suggests that for temperatures below 15 K it is possible to assume an absorbance spectrum like the one measured at 15 K. The $\lambda_{cut-off}$ results to be about 325 nm at room temperature and about 305 nm for $T < 15$ K.

Also the refractive index shows a temperature dependence, but as for the absorption length no reference is available in literature. Nevertheless the variation is expected to follow the absorption length one (a shift of about 20 nm toward lower wavelengths). But, unlike the absorption length, the temperature dependence of the refractive index weakly affects the number of Cherenkov photons emitted (less than 1%), therefore it can be neglected.

2.2 Number of Cherenkov photons emitted per unit path length

Using the refractive index and the absorption length, it is possible to evaluate the number and the wavelength spectrum of the emitted Cherenkov photons per unit path length of the charged particle.

As an example, we computed the number of Cherenkov photons produced by an electron of 2.5 MeV (as this energy is close to the 0 ν DBD Q-value) for 1 mm path length. The energy of this electron is well above the threshold for Cherenkov emission: 50 keV using $n_o(400 \text{ nm}) = 2.44$. For comparison, the threshold for α particles would be 400 MeV.

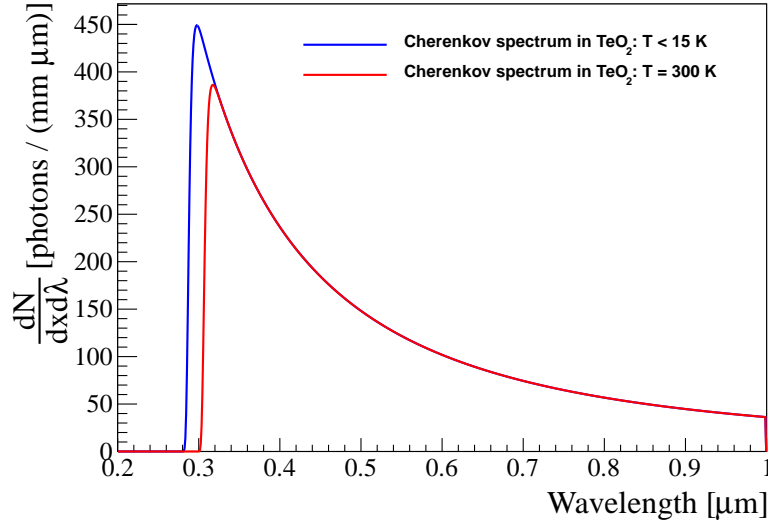


Fig. 3. Emission spectrum of the Cherenkov photons in TeO₂ crystal at room temperature and at cryogenic temperature ($T < 15$ K). These spectra are evaluated using an electron of about 2.5 MeV for 1 mm path length.

The number of photons emitted by the 2.5 MeV electron was computed integrating Eq. 1 in the wavelength domain. The lower limits was set to 200 nm, well below the beginning of the absorption range (see Fig. 2). Since most of the optical properties required for the simulation of the photons propagation are available up to 1000 nm, we chose this value as upper limit for the integration. We estimated that this approximation accounts for the 93% of the total energy emitted by Cherenkov effect, enough for the purpose of the simulation presented in this paper. Integrating Eq. 1 using $n_o(\lambda)$ ($n_e(\lambda)$) resulted in a number of emitted Cherenkov photons of 84.1 photons/mm (86.5 photons/mm). At cryogenic temperature the $\lambda_{cut-off}$ decreases to about 20 nm resulting in an increase of the Cherenkov photons up to 92.9 photons/mm (95.5 photons/mm) using $n_o(\lambda)$ ($n_e(\lambda)$). The room temperature spectrum of emitted Cherenkov photons compared with the low temperature one is shown in Fig. 3.

The TeO₂ stopping power for electrons can be found in [16]: thanks to this parameter it is possible to perform a raw approximation of the number and energy of Cherenkov photons produced by an electron with a kinetic energy of about 2.5 MeV. With a dE/dx of about 0.8 MeV/mm its path results in 3 mm, corresponding to an average number of Cherenkov photons equal to ~ 280 and an energy of about 780 eV. On the contrary, as mentioned in Sec. 1, the Cherenkov energy actually detected is only 100 eV.

3 Light trapping and surface effects of tellurium dioxide crystal

The number of photons able to come out from the TeO₂ crystal is smaller than 280; this is due to the light trapping that happens when an optical photon travels from a medium with a higher refractive index (n_1) to one with a lower refractive index (n_2). If the incident angle of the photon on the crystal surface is greater than $\theta_{Critical} = \arcsin(n_2/n_1)$ the photon is reflected inside the crystal. For the TeO₂ surrounded by vacuum $\theta_{Critical}$ is shown in Fig. 1 for both ordinary and extraordinary refractive index. This small critical angle added to the high symmetry of the cubic shape of the crystal leads to a high probability that photons are internally reflected an indefinitely large number of times, i.e. they remain trapped inside the crystal until absorption.

Fortunately, this trapping effect can be partially overcome thanks to the roughness of the crystal surface and the birefringence of TeO₂. Both these properties can randomly change the reflection angle increasing the exit probability of the photons, as will be shown in Sec. 5.

4 Comparison between Monte Carlo simulation and data

As roughly evaluated in section 2, the produced Cherenkov light for 2.5 MeV electron amounts to about 780 eV, a very different value from the 100 eV measured in Ref. [10]. In order to understand this discrepancy we developed a detailed Monte Carlo simulation able to reproduce the Cherenkov photons production and propagation inside the experimental set-up. The simulation was split in two parts: the total number of emitted Cherenkov photons was evaluated using

Geant4, the propagation of these photons inside the different components of the experimental set-up was reproduced by means of Litrani [17], a general simulation software specifically developed for the propagation of optical photons.

The Monte Carlo starts with the simulation of the three γ s that produce the six most intense peaks in the TeO₂ energy spectrum (see Ref. [9,10] for more details): 2615 keV, 1460 keV and 911 keV respectively emitted by ²⁰⁸Tl, ⁴⁰K and ²²⁸Ac. The γ emitted by ²⁰⁸Tl produces the 2615 keV photo-peak and two additional peaks: the single and double escape peaks, in which respectively one or two 511 keV γ escapes from TeO₂ crystal after an $e^+ + e^-$ annihilation. If the $e^+ + e^-$ annihilation occurs in the inert materials or in a neighbour crystal, the 511 keV γ can interact with the TeO₂ bolometer producing the 511 keV γ photo-peak.

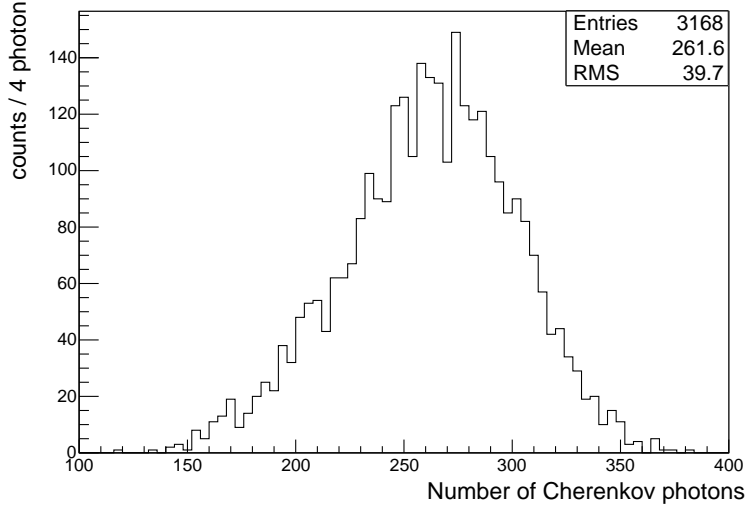


Fig. 4. Distribution of Cherenkov photons produced by the 2615 keV γ interactions that have released all their energy in the crystal.

Selecting, for example, the events in the ²⁰⁸Tl photopeak it is possible to know the kinetic energy and the path of all electrons and positrons produced in these interaction and, using Eq 1, assess the number of Cherenkov photons produced by each e^\pm particle with a kinetic energy greater than 50 keV, as shown in Fig. 4. Once the number of Cherenkov photons produced is known, it is possible to simulate their propagation in the experimental set-up with Litrani; since the refractive index and the absorption length of germanium disk [18] and the real and imaginary part of the refractive index of VM 2002 reflective foil [17] have been found in literature only at room temperature, the cryogenic optical properties for these materials are approximated with the room temperature values.

Focusing the attention on the ²⁰⁸Tl photopeak the light produced by 100 of these interactions are simulated: for each interaction the total number of Cherenkov photons and their wavelength distribution are randomly generated respectively according to the distribution shown in Fig. 4 and Fig. 3. The average energy emitted results in about 744 eV, in agreement with the raw approximation performed in Sec. 2.

Each Cherenkov photon is propagated through the materials until it is absorbed: if it is absorbed inside the germanium disk it is considered as detected. The number of detected photons and their wavelength distribution for the ²⁰⁸Tl peak are shown in Fig. 5.

The total Cherenkov energy absorbed by the germanium light detector can be evaluated integrating the spectrum of Fig. 5 (right), resulting in 117.8 eV per interaction. The same procedure is applied to the other five peaks and the average energies detected are compared with the ones measured [10] in Fig. 6.

The simulation well reproduces the experimental data (see Ref. [10] for the detector set-up details) and confirms that the Cherenkov light detected is only 18% of the produced one: the number of photons escaping from the unwrapped crystal face are 27% of the created one and, due to the reflectivity of the germanium, only 69% of them are actually absorbed by the light detector. The remaining photons are absorbed by the TeO₂ crystal (60%) and by the reflective foil and by the LD copper frame (22%). Similar results were found simulating with the Monte Carlo other reflectors as PTFE tape or aluminum foil. This confirms that no significant improvement in light collection can be achieved using these reflectors instead of VM 2002.

In light of these considerations it is possible to understand why all the trials to increase the light collection efficiency were not successful: the trapping effect of the TeO₂ crystal and the reflectivity of the germanium disk do not allow to collect more than the 18% of the Cherenkov energy produced in the β/γ interactions. This explains the reason why

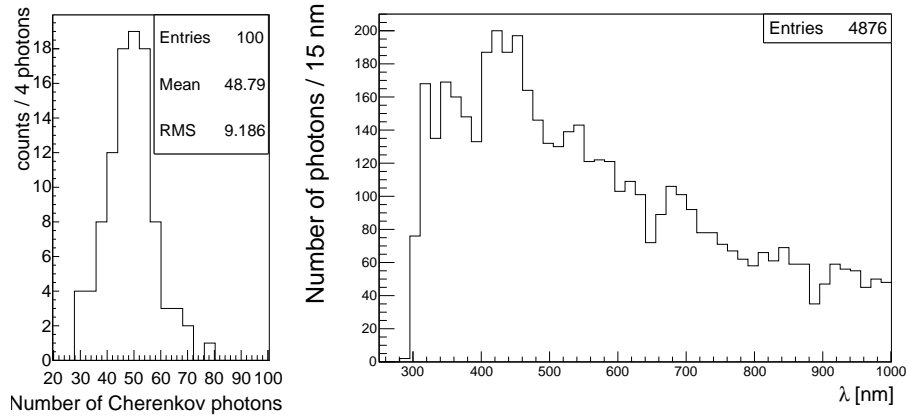


Fig. 5. Distribution of the number of Cherenkov photons (left) and their wavelength distribution (right) absorbed by the germanium disc in one hundred 2615 keV γ -interactions simulated by means of Litran. The reduction of photons detected by the light detector between $300 \div 400$ nm is due to the low reflectance efficiency of the VM 2002 reflective foil in that wavelengths range.

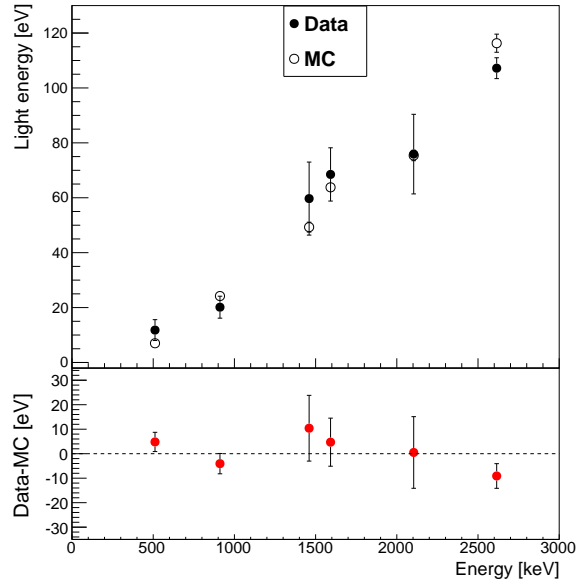


Fig. 6. Energy release as measured from Ref. [10] (solid black circles) and simulated (open black circles) energy release in the Ge LD. In the bottom the red dots represent the subtraction between data and Monte Carlo.

the only test in which more than 110 eV at the ^{208}Tl line were detected was the test performed with a smaller TeO_2 crystal for which the self light absorption is smaller (see Ref. [9]).

The Monte Carlo results are fairly dependent on the only free parameter of the simulation, θ_{rough} , parameterizing the surface roughness of the crystal. A detailed study of the light emitted as function of θ_{rough} will be shown in the next sections.

To test the validity of the Monte Carlo despite the unavoidable approximations discussed in Sec. 2.2 and 4 an additional cross-check was made: the LY measurement performed using the smaller TeO_2 crystal doped with samarium was entirely reproduced exploiting the Monte Carlo (see Ref [9] for a complete set-up description). The light measured at the ^{208}Tl line was found to be 195 ± 7 eV and the simulated one 205 ± 4 eV, in very good agreement with the data. This result can be considered as a further evidence that, despite the approximations performed, the Monte Carlo simulation developed in this work is able to reproduce and predict the Cherenkov light yield of TeO_2 bolometers.

5 Effect of the crystal surfaces roughness on light yield

As anticipated, the only free parameter of the simulation is θ_{rough} which parametrizes the surface roughness of the crystal. The surface treatment of the CUORE crystals was developed to maximise the surface radio-purity of the crystal. Due to TeO₂ hardness characteristics, the surface treatment results in two opposite faces with polishing quality close to optical polishing grade, and the remaining four faces featuring a higher roughness. The crystal surface therefore is not optimized for the light collection. In the measurements performed in Ref. [9,10] the germanium light detector monitors one of the two polished faces of the crystal.

The simulation developed in this work reproduces all data collected using a surface roughness for the four later faces corresponding to $\theta_{rough} = 20^\circ$. As discussed in Sec. 3 the surface roughness interferes with the trapping effect produced by the high refractive index and symmetry of TeO₂ bolometer, increasing the photons emission probability. The result shown in Fig. 7 highlights the correlation between the emitted light and the surface roughness of the crystal faces. In Fig. 7 is also reported the value of θ_{rough} that reproduces all the cryogenic tests performed on cubic TeO₂

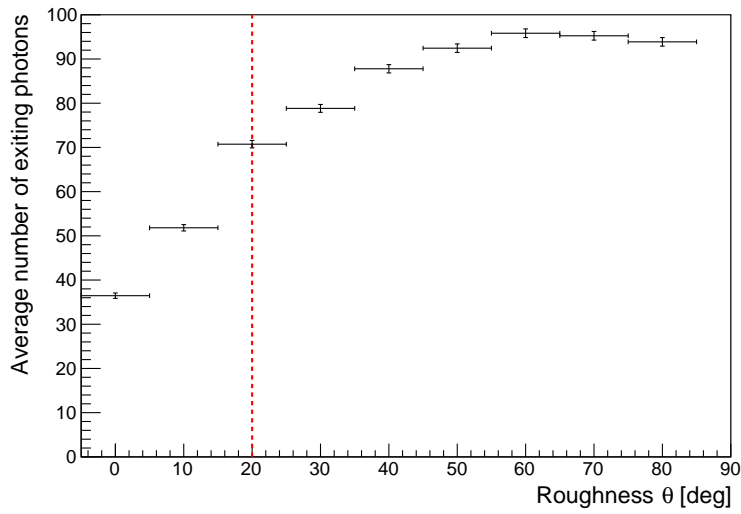


Fig. 7. Average number of photons for interaction that reach the LD plane (1.2 cm from the crystal face) as function of the roughness of the four later crystal faces.

crystal (red dotted line).

The simulation suggests that the LY can be maximized increasing the roughness of the four lateral faces of the crystal. With respect to the standard CUORE TeO₂ crystal the light yield can be increased by a factor 35%. No differences were found assuming that also the two opposite polished faces of the TeO₂ crystal are rough: the results are compatible with the ones shown in Fig. 7, suggesting that no additional advantage can be obtained.

6 Improving the light collection

In addition to the increase of the lateral surface roughness also the shape of the germanium light detector can be optimized in order to maximize the light collection efficiency. In Ref. [10] the germanium light detector was a disk of 5 cm in diameter, 300 μm thick; obviously the best shape and size for the germanium light detector is the one that matches the TeO₂ face: the new light detector that was simulated is a $5 \times 5 \text{ cm}^2$ and 300 μm thick germanium slab. Thus the active surface of the LD increases by 21%. The distance between the crystal face and the germanium slab does not seem to produce a significant increase in the light collection efficiency in the range between 1.2 and 0.2 cm (in the hypothesis that the reflective foil is applied also on the empty space between the crystal face and the LD plane), and for simplicity it was set to 1 cm. Using the same procedure adopted in section 4 it was possible to evaluate the expected Cherenkov energy for the six most intense peaks of TeO₂ spectrum (511 keV, ²²⁸Ac, ⁴⁰K, single escape, double escape and ²⁰⁸Tl) in the new optimized experimental set-up: the mean light from the γ peaks was fitted with a line and an $E_{th} = 327 \pm 18 \text{ keV}$ and a $LY = 72 \pm 1 \text{ eV/MeV}$ (see Fig. 8) was obtained. The optimized set-up should be able to increase the TeO₂ LY of about 58% respect to the one measured in Ref. [10].

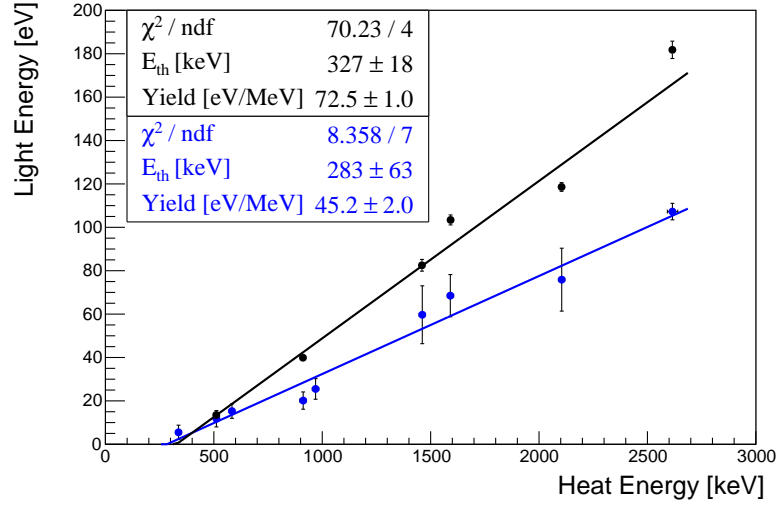


Fig. 8. Comparison between the Cherenkov energy simulated in the optimized set-up as a function of the energy released in the TeO₂ bolometer (black line and solid circles) and the measured one in the set-up used in Ref. [10]. The high value of the fit χ^2/ndf for the simulation can be explained by the fact that the first order polynomial function is just a first approximation of the real trend of the Cherenkov energy as function of the γ interaction in TeO₂ bolometer, as explained in the text.

7 β/γ discrimination

From Fig. 8, we can recognize that the linear function used in Ref. [9,10] to quantify the Cherenkov LY of TeO₂ bolometers is just a first approximation of the real trend of the Cherenkov energy as function of the energy released in TeO₂ by β/γ interaction. For example, the events produced by the double escape peak (1593 keV) are $e^- + e^+$ interactions that produced an average Cherenkov energy slightly greater than a γ interaction with energy 1593 keV; similarly, the events produced by the single escape peak (2104 keV) are $e^- + e^+ + \gamma(511 \text{ keV})$ and, as expected, the Cherenkov energy obtained is equal to the one obtained for the double escape peak plus the Cherenkov energy obtained for the 511 keV gamma interaction, and results slightly smaller than a γ interaction with energy 2104 keV. Also for the 2615 keV peak a small deviation from the linear trend seems present. Given these considerations it seems

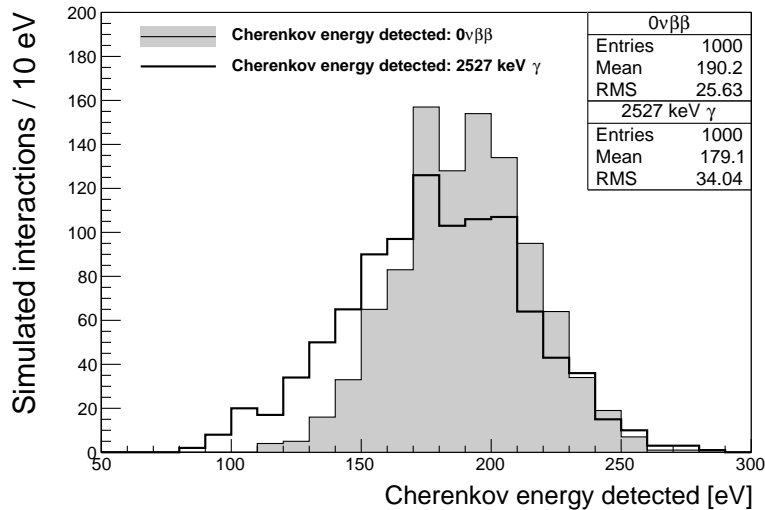


Fig. 9. Energy distributions of the Cherenkov light produced by 1000 $0\nu\text{DBD}$ events of ^{130}Te and 1000 γ interaction with the same energy. The intrinsic fluctuation of these energy deposition are produced by the Poisson fluctuation of the number of emitted photons and by the dE/dx fluctuation of the electrons paths.

that a β interaction and a γ one with the same energy produce a different Cherenkov yield. In order to study if also

the γ background can be removed from TeO₂ bolometers the Cherenkov energy detected by the optimized set-up is simulated for $0\nu\text{DBD}$ events of ^{130}Te (two electrons with a total kinetic energy of 2.527 keV) and then compared with the one produced by γ interactions with the same energy. The two energy distributions detected by the germanium slab are compared in Fig. 9: even if the average number is different the distributions are almost completely overlapped therefore, thus preventing a discrimination between β and γ interactions.

8 Conclusions

In this paper a complete simulation of the Cherenkov photons production and propagation in TeO₂ bolometers is presented. The results are compared with the data presented in Ref. [9,10] and a good agreement was found. The simulation also suggests that, increasing the lateral surface roughness of the crystal and optimizing the size and shape of germanium LD, the Cherenkov energy detectable at $0\nu\text{DBD}$ of ^{130}Te will reach 190 eV. Also the possibility to perform a β - γ discrimination was investigated but, the intrinsic fluctuation of the number of Cherenkov photons does not allow such kind of particle identification.

Acknowledgements

I would like to thanks Dr. Ioan Dafinei for the great help in providing the transmission measurement of TeO₂ crystal and Dr. Marco Vignati for the continuous support offered in the realization of this work. This work was supported by the Italian Ministry of Research under the FIRB contract no. RBFR1269SL.

References

1. D.R. Artusa, et al., Adv. High Energy Phys. **2015**, 879871 (2015). DOI 10.1155/2015/879871
2. G. Wang, et al., (2015)
3. F. Bellini, N. Casali, I. Dafinei, M. Marafini, S. Morganti, F. Orio, D. Pinci, M. Vignati, C. Voena, JINST **7**, P11014 (2012). DOI 10.1088/1748-0221/7/11/P11014
4. N. Casali, F. Bellini, I. Dafinei, M. Marafini, S. Morganti, F. Orio, D. Pinci, M. Vignati, C. Voena, Nucl. Instrum. Meth. **A732**, 338 (2013). DOI 10.1016/j.nima.2013.07.024
5. F. Bellini, et al., JINST **5**, P12005 (2010). DOI 10.1088/1748-0221/5/12/P12005
6. T. Tabarelli de Fatis, Eur.Phys.J. **C65**, 359 (2010). DOI 10.1140/epjc/s10052-009-1207-8
7. F. Bellini, et al., JINST **9**(10), P10014 (2014). DOI 10.1088/1748-0221/9/10/P10014
8. J. Beeman, F. Bellini, N. Casali, L. Cardani, I. Dafinei, et al., JINST **8**, P07021 (2013). DOI 10.1088/1748-0221/8/07/P07021
9. J. Beeman, F. Bellini, L. Cardani, N. Casali, I. Dafinei, et al., Astropart.Phys. **35**, 558 (2012). DOI 10.1016/j.astropartphys.2011.12.004
10. N. Casali, et al., Eur. Phys. J. **C75**(1), 12 (2015). DOI 10.1140/epjc/s10052-014-3225-4
11. P.A. Čerenkov, Phys. Rev. **52**, 378 (1937). DOI 10.1103/PhysRev.52.378. URL <http://link.aps.org/doi/10.1103/PhysRev.52.378>
12. N. Uchida, Phys. Rev. B **4**, 3736 (1971). DOI 10.1103/PhysRevB.4.3736. URL <http://link.aps.org/doi/10.1103/PhysRevB.4.3736>
13. W. Sellmeier, Ann. Phys. Chem. pp. 143–271 (1871)
14. T. Takizawa, Journal of the Physical Society of Japan **48**(2), 505 (1980). DOI 10.1143/JPSJ.48.505. URL <http://dx.doi.org/10.1143/JPSJ.48.505>
15. B.R. Sahu, L. Kleinman, Phys. Rev. B **69**, 193101 (2004). DOI 10.1103/PhysRevB.69.193101. URL <http://link.aps.org/doi/10.1103/PhysRevB.69.193101>
16. M.Z. M.J. Berger, J.S. Coursey, J. Chang. Estar, pstar, and astar: Computer programs for calculating stopping-power and range tables for electrons, protons, and helium ions (version 1.2.3) (2005). URL <http://physics.nist.gov/Star>
17. F.X. Gentit, Nuclear Instruments and Methods in Physics Research Section A: Accelerators, Spectrometers, Detectors and Associated Equipment **486**(1–2), 35 (2002). DOI [http://dx.doi.org/10.1016/S0168-9002\(02\)00671-X](http://dx.doi.org/10.1016/S0168-9002(02)00671-X). URL <http://www.sciencedirect.com/science/article/pii/S016890020200671X>. Proceedings of the 6th International Conference on Inorganic Scintillators and their Use in Scientific and Industrial Applications
18. D.E. Aspnes, A.A. Studna, Phys. Rev. B **27**, 985 (1983). DOI 10.1103/PhysRevB.27.985. URL <http://link.aps.org/doi/10.1103/PhysRevB.27.985>